

Improving flash flood risk assessment using a simple approach for extreme rainfall scaling and storms transposition

Marco Lompi^{1,2}  | Enrica Caporali¹  | Luis Mediero²  | Bernardo Mazzanti³

¹Department of Civil and Environmental Engineering, University of Florence, Florence, Italy

²Department of Civil Engineering: Hydraulic, Energy and Environment, Universidad Politécnica de Madrid, Madrid, Spain

³Civil Protection Service of Tuscany Region, Florence, Italy

Correspondence

Marco Lompi, Department of Civil and Environmental Engineering, University of Florence, Florence, Italy.
Email: marco.lompi@unifi.it

Abstract

Flash flood risk management is among the key topics of the European Flood Directive. Design hydrographs of small river basins could underestimate the hydraulic risk in case of intense and short-duration events because of the intensification of hourly rainfall and the design rainfall depths uncertainty in often ungauged river basins. The use of synthetic hyetographs obtained from past observed events can be useful for a better evaluation of the flash flood hazard at the river basin scale. For this reason, a simple approach based on rainfall scaling and storms transposition of occurred events is presented to identify areas where design discharges underestimate the flash flood risk. The methodology considers the spatial distribution of the observed storms over a specific zone and the areal reduction factors to scale the observed hyetographs for different river basins extensions. Hyetographs of past observed events are used as input of a hydrological model in a set of river basins located in Northern Tuscany (Italy). The results show how peak discharges of short-duration events are usually greater than the design floods of the small river basins with an area generally less than 30 km².

KEYWORDS

extreme events, flash floods, hydrological modeling, risk assessment

1 | INTRODUCTION

Flash floods are considered among the worst natural hazards, as they are characterized by sudden, short-duration heavy rains, and unpredictable peak discharges (Ali et al., 2017). Flash floods are generated by rainfall events, mainly of convective origin, that occur locally and usually impact small river basins with response times of a few hours or less (Marchi et al., 2010).

In the last three decades, the number of significant flood events in the world has increased, and this is related to the impact of climate change on extreme precipitation and with the land use change connected with the increasing urbanization (Kourgialas & Karatzas, 2011).

Climate change is leading to the intensification of extreme rainfall. High precipitation quantiles of short durations generally increase with temperature as this is

This is an open access article under the terms of the Creative Commons Attribution License, which permits use, distribution and reproduction in any medium, provided the original work is properly cited.

© 2022 The Authors. *Journal of Flood Risk Management* published by Chartered Institution of Water and Environmental Management and John Wiley & Sons Ltd.

possibly related to an increase of convective origin precipitation (Berg et al., 2013; Lenderink & Van Meijgaard, 2008).

Moreover, flash floods are expected to increase in the future in frequency and magnitude under some climate change scenarios (Dougherty & Rasmussen, 2021; Zhang et al., 2019), and increasing trend of flash flood events have been detected in the Mediterranean area (Esposito et al., 2018; Llasat et al., 2016). Consequently, there is a need for effective approaches and methods for flash flood management under such changing circumstances (Dawod et al., 2011).

Southern Europe is vulnerable against flash flood events because their intensity is greater in magnitude in the Mediterranean countries and decreases moving inland (Gaume et al., 2009). Indeed, in the last few years, a great number of flash floods have occurred near the Tyrrhenian Sea, along the coasts of Liguria and Tuscany (Arrighi & Castelli, 2020; Faccini et al., 2015, 2018). In this context, decision-makers need a simple and useful approach to take the right measures against the impacts of these events. Nevertheless, observed data about flash floods are scarce, as such events often occur in small ungauged river basins (Blöschl et al., 2019).

The risk associated with flash flood can be reduced with forecasting models that work in real time to give a forewarning, such as the Flash Flood Guidance (Mogil et al., 1978). At the same time, flash flood risk pre-assessment, that is, the identification of the prone areas to flooding, can support decision-making and reduce the hazard of these events (Cao et al., 2016; Saharia et al., 2017).

The objective of this work is to define a simple methodology to provide synthetic hyetographs that can be used in hydrological models to identify river basins with design discharges that underestimate the flash flood risk. This is particularly relevant to areas where design rainfall depths are affected by a greater uncertainty due to short-time series length, as well as for ungauged river basins.

The synthetic hyetographs are determined with a simple approach by scaling past observed event hyetographs with the areal reduction factors (ARF) on different river basins sizes. The hyetographs are then used in rainfall-runoff models with a stochastic storm transposition (SST). Franchini et al. (1996) did a similar attempt by coupling the SST with rainfall runoff modeling to estimate the exceedance probabilities of design floods. A similar attempt was carried out by Nnadi et al. (1999), where a comparison was made between the design storms and occurred events to understand if a set of different hydrological models overestimate or underestimate the risk of short duration storms. In this work, the proposed methodology is meant for the decision-makers that must

assess flood risks in the river basin authorities and has the goal to improve the prediction of flash flood risk only, by adapting the design discharges that are commonly used in each area. Therefore, the scaling procedure based on the ARFs is applied to extreme short-duration events (SDEs) only.

The ARF has been defined by the Natural Environmental Research Council (NERC) in the Flood Studies Report (NERC, 1975) and represents the factor that if applied to point rainfall for a specified duration and return period, gives the areal rainfall for the same duration and the same return period (De Michele et al., 2001). The ARF can be obtained in two different ways: a fixed-area approach, which focuses on the rain gauge sites within a fixed-area like a watershed, and a storm-centered approach, in which the area considered is not fixed but varies depending on specific rainfall events (Kim et al., 2019). Many empirical and analytical methods have been developed for estimating ARFs (Bacchi & Ranzi, 1996; Barbero et al., 2014; Pavlovic et al., 2016). Sivapalan and Blöschl (1998) note that storm-centered ARFs are usually smaller than geographically fixed ARFs, and this is probably due to convective events of a limited area.

The storm-centered approach is used here, and the hyetograph recorded by the rain gauge with the maximum rainfall depth within an event is scaled with the ARFs on different river basin sizes.

The obtained hyetographs are then applied on other locations with an SST. SST is described in Wright et al. (2020) as the process that involves resampling and transposing (i.e., geographically moving in the zonal and meridional directions) storm events to generate hypothetical events from a collection of realistic events.

The synthetic hyetographs obtained by the past events can only be tested on the river basins with a similar rainfall statistical distribution of the place in which the events occur. In this way, they are tested over catchments that can statistically have similar events, avoiding unreal comparison with the design hydrographs. Fofoula-Georgiou (1989) defined the storm transposition area (STA) as the area within which all the occurred storms can be transposed anywhere with the same occurrence probability but with an adjustment to their depth. Indeed, in homogeneous regions, storms are expected to have similarities in their internal structure despite their different durations and total rainfall depths (Koutsoyiannis & Fofoula-Georgiou, 1993).

The methodology is applied in Northern Tuscany (central Italy). The derivation of synthetic hyetographs is made by scaling recent short duration events occurred in the area. The hyetographs are used to identify where the design discharges used in the region underestimate the

flash flood risk, even if several studies based on trend analysis of observed precipitation highlighted that there is no evidence of changes in the precipitation intensity or extreme events frequency in this area (Caporali et al., 2021). The aim of the study is to understand if the design events are precautionary also in depicting the flash flood risk and how, if needed, they could be adjusted. Indeed, the results of the comparison between SDEs and design floods are summarized introducing the use of a delta flash flood design index (ΔFFD), which represents the ratio between the mean of all the peak discharges of the selected SDEs and the design event peak.

2 | METHODOLOGY

The methodology is purposefully applied at the regional scale to improve the flash flood hazard assessment on a set of small river basins. The methodology is composed of five steps: selection of the most extreme SDEs based on rainfall data (Section 2.1), spatial distribution of the selected events (Section 2.2) to calculate the ARFs (Section 2.3), hydrological modeling (Section 2.4), and comparison of the selected events with the design hydrographs in a set of small river basins (Section 2.5).

2.1 | Selection of the most intense short-duration events

The most intense events that have occurred over a large region are selected using rainfall data rather than discharge data because it is recognized that some isolated heavy rainfall may not cause extreme runoff to impact discharge measurement (Svensson & Jones, 2010). Furthermore, since flash flood events are usually consequential to extreme rainfall within a few hours, the selection is made to identify only SDEs. An SDE is defined in this study as an event with at least 80% of the total rainfall within 3 h. For this reason, to analyze if an event fulfills the definition of SDE, a dataset with at least a 15-min time step is required. The analysis is focused on rainfall data, regardless of whether the rainfalls generate a flash flood. Indeed, some SDEs can occur over large river basins without flood damages despite a great rainfall intensity or runoff. The SDEs have been selected analyzing maxima rainfall in the duration of 3 h. Without normalization of the maxima rainfall, the SDEs are found only in the rainiest part of the study area. For this reason, the events have been selected with the highest values of rainfall depths standardized with the design rainfall depth for a given return period, in this case 200 years (Equation 1) as

$$h_n = h_{ev}/h_{200} \quad (1)$$

where h_n is the normalized rainfall depth, h_{ev} is the measured precipitation, and h_{200} is the design rainfall depth at the rain gauge location. The normalization must be done considering the same duration, that is, h_{ev} and h_{200} are the SDE depth recorded by a rain gauge and the design rainfall depth, respectively, in the same location and for the same duration. Selecting the event with the normalized rainfall depth, the frequency of a given event can be estimated, contextualizing it with the place in which it occurs and comparing it with the values commonly used in the hydrological models in the same area. All the events that are found with the normalized rainfall depth that do not fulfill the SDE definition are not considered. Sometimes, more than one rain gauge recorded the same SDE and as such entered in the classification more than once. In these cases, only the hyetograph of the rain gauge with the maximum value is considered for the scaling procedure. Hence, the obtained hyetographs associated to a given SDE have the same shape, but their intensity changes with the river basin area of the catchment on which the real event is modeled. Since the selected events must be applied only to areas with similar design rainfall depths a set of SDEs must be found for each STA to avoid meaningless comparison between occurred and design hydrograph. Moreover, the number of selected events for each STA is estimated with a peak over threshold on the normalized rainfall depth h_n . The threshold is set equal to 0.9 to identify the most extreme SDEs occurred in the area.

2.2 | Spatial distribution of the selected events

After the identification of the most intense SDEs, the selected hyetographs have been scaled using a spatial analysis. For each event, all the rain gauges around the one with the maximum rainfall with a rainfall depth greater than 1 mm have been considered in the analysis. Spatial rainfall distributions are estimated with the inverse distance weighting method (IDW) (Equations 2 and 3) as

$$h(x) = \begin{cases} \frac{\sum_{i=1}^N w_i(x) h_i}{\sum_{i=1}^N w_i(x)}, & d(x, x_i) \neq 0 \\ h_i, & d(x, x_i) = 0 \end{cases} \quad (2)$$

where

$$w_i(x) = \frac{1}{d(x, x_i)^p} \quad (3)$$

In the previous equations, h is the total rainfall depth in a given location x , h_i is the total rainfall depth recorded at the gauging site x_i , w_i is the weight for the rainfall recorded at the gauging site i , $d(x, x_i)$ is the Euclidean distance between a given point x and the rain gauging site i , and p is a power parameter that is set equal to two.

The selected events are often convective storms. Consequently, they are spatially localized, and the number of rain gauges considered for each event is usually very small. For this reason, this methodology works well only if the spatial information density of the rain gauge network of the study is high, with indicatively at least a rain gauge every 100 km². The Kriging method has not been used to interpolate observations because of the small number of semivariance values for the construction of the semivariogram. Sometimes, SDEs can cover a larger scale, though they always show a reduced area where the highest rainfall intensities are concentrated. Rainfall spatial distributions are gridded to simplify the procedure as explained in the next section.

2.3 | ARFs computing

Areal reduction factors are computed for each SDE with the spatial distribution obtained in the previous section to scale the rainfall event over different catchment areas. The punctual intensity recorded in the rain gauge with the maximum value is reduced and distributed on a given area with the ARF. In this study, a specific river basin is not considered in the same way as in the fixed-area approach. The ARF is calculated just for a generic extension that is centered in the storm and indicates how much the average rainfall depths change on different storm-centered surfaces, becoming smaller as area increases. It represents the highest probability to find greater precipitation values nearby the rain gauge with the maximum rainfall value and decreasing intensities with increasing distances to the storm center.

Since the cells of the rainfall spatial distribution have the same area, there is a biunique correspondence between a generic river basin area and the number of cells that must be analyzed. For instance, setting the cell size equal to 100 m, the ARF for a river basin of 20 km² is calculated by finding the 2000 neighboring cells with the greater values in the grid and calculating the average depth on those cells for that area. Indeed, the identification of the storm center within the raster grid is made by looking for the maximum average rainfall depth for a given area. As such, the storm

center location can change for different considered areas. In the study, all the groups are square aggregations of cells; hence, the intensity of the field is averaged over a box of size $L \times L$ centered around a given location (i, j) as in Venugopal et al. (1999). The choice of a fixed shape is useful to guarantee a unique ARF associated to a specific event and to a generic extension. Therefore, the hyetograph of a given event is scaled with the same ARF for all the river basins with the same area.

The entire rainfall raster can be considered a square matrix, whereas the square aggregation of neighboring cells are submatrices. Therefore, all the possible combinations of cell groups with a given dimension can be calculated. If the entire raster is a square matrix $A(k \cdot k)$, the number of possible submatrices within the raster with m cells on their side is equal to n^2 , where n is:

$$n = k - m + 1 \quad (4)$$

Figure 1 shows an example for a square raster with 25 cells ($k = 5$), considering two hypothetical catchment areas. With m equal to three, there are nine possible submatrices with an area of nine cells. With m equal to four, there are four submatrices with an area of 16 cells.

The average rainfall depth is calculated for each submatrix, obtaining the ARF by using Equation (5):

$$\text{ARF} = H_a / H_{\max} \quad (5)$$

where H_a is the greatest average rainfall depth within the set of all n^2 possible sub-matrices with a given dimension m , and H_{\max} is the maximum value recorded by the rain gauge. The rainfall depth H_{\max} is different from h_{ev} in Equation (1) because it represents the total precipitation of the event, not the maximum value recorded in the given duration (3 h).

To find the maximum average rainfall depth H_a within the entire raster $A(k \cdot k)$, a matrix $B(n \cdot n)$ is composed of the average values for each submatrix.

$$B(i, j) = \frac{\sum_i^{m+i-1} \sum_j^{m+j-1} A(i, j)}{m^2} \quad (6)$$

where $B(i, j)$ represents the average of all the elements belonging to the submatrix $S(i, j)$ with its (1,1)-element in the i -th row and j -th column of the matrix A , and m is the number of cells in the submatrix side.

Continuing with the previous example, the average value of the gray submatrix $S(4,3)$ (Figure 2), with its (1,1) element in the fourth row and third column of matrix A can be calculated by Equation (7):

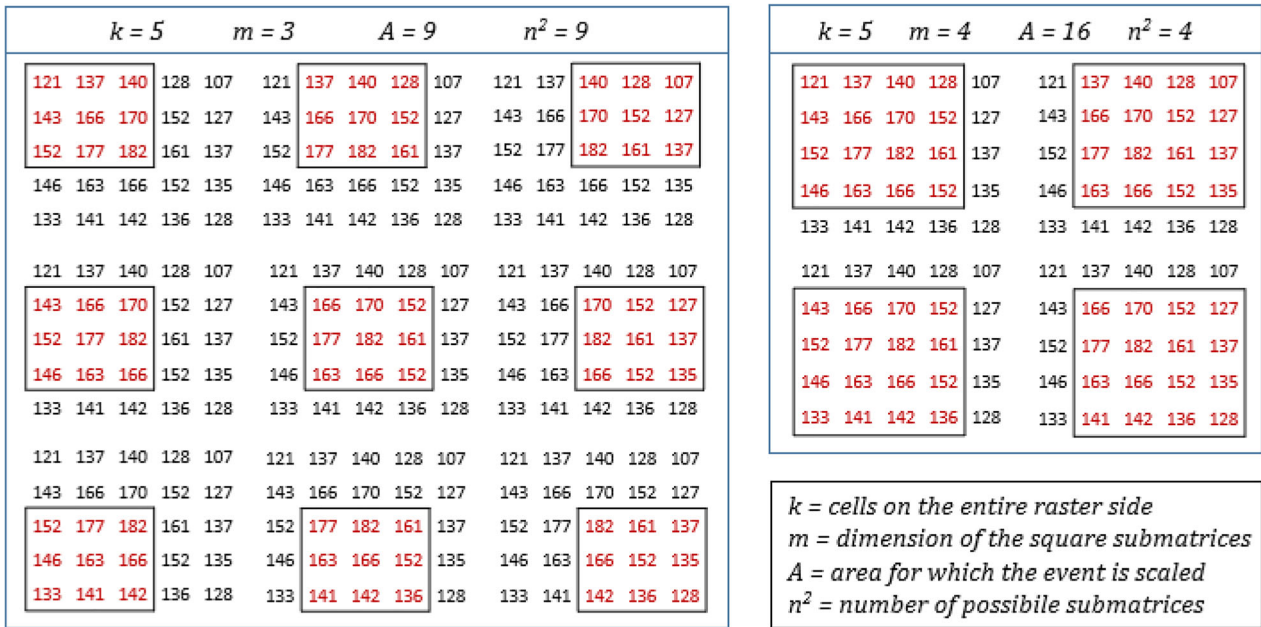


FIGURE 1 Example of all the possible combinations of submatrices with a given dimension ($m \cdot m$) within the same rainfall raster ($k \cdot k$)

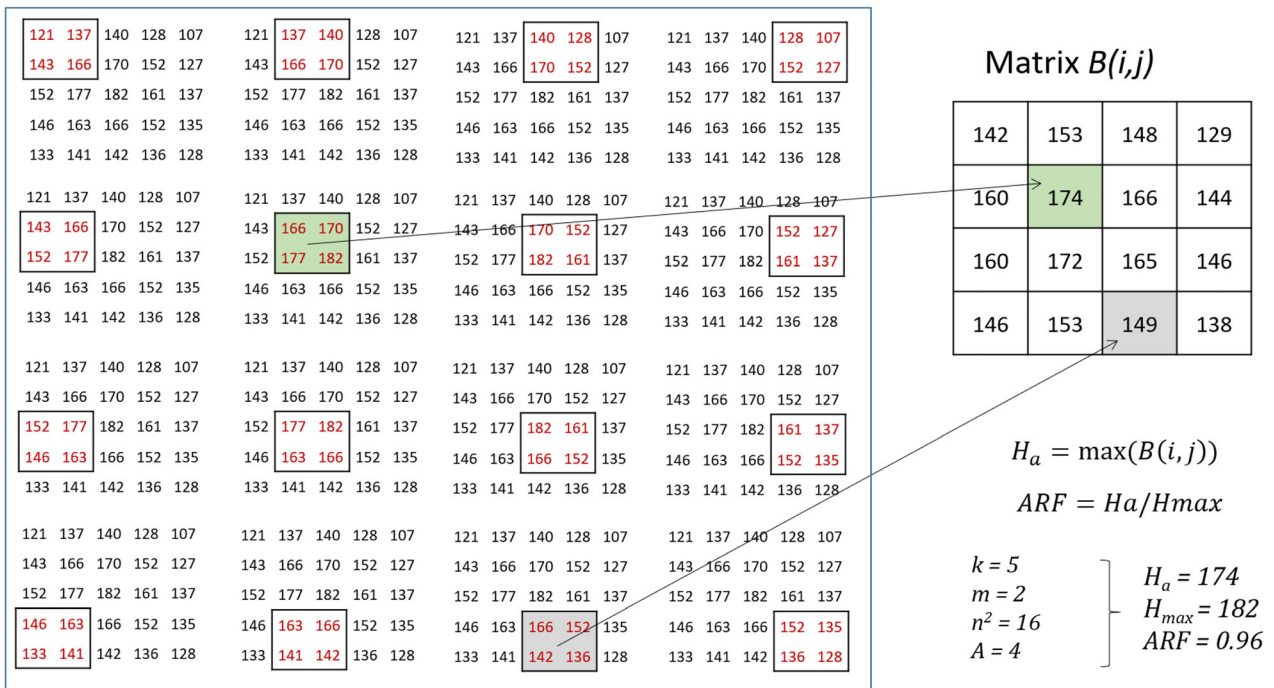


FIGURE 2 Evaluation of the maximum average rainfall depth H_a to calculate the areal reduction factor for river basins with an area of four cells

$$B(4,3) = \frac{\sum_4^{2+4-1} \sum_3^{12+3-1} A(i,j)}{2^2} = \frac{\sum_4^5 \sum_3^4 A(i,j)}{4} = \frac{[A(4,3) + A(4,4) + A(5,3) + A(5,4)]}{4} \quad (7)$$

The greatest element of the matrix B is H_a , that is the maximum average rainfall depth for that given area. In the example (Figure 2), the maximum average value corresponds to the green submatrix $S(2,2)$, where the storm center is located, obtaining $H_a = 174$ mm. H_{max} is the

maximum value of matrix A , i.e. $H_{\max} = 182$ mm. Using Equation (5), ARF = 0.96 for a catchment area composed of four cells.

Each SDE is represented with the hyetograph recorded at the rain gauge station with the maximum within the event and a set of ARF values associated with the river basin areas in which it must be tested.

2.4 | Hydrological modeling

A hydrological model is used to compare the hydrographs generated by both the SDEs and the design events. The goal is to use the obtained hyetographs only on the river basins that can have similar rainfall statistics, moving them just nearby the location in which they really occur within the same STA. In the proposed methodology, the SDEs are tested on the river basins with a design rainfall greater than the one at the location of the occurred event. The logic is that “if an event occurred in a certain location, it is likely to occur also where the design rainfall depths are greater.”

A semi-distributed hydrological model is applied, as the hyetographs with the ARFs already consider the spatial distribution of the precipitation and give a measure of the average precipitation over a river basin. In addition, a semi-distributed hydrological model is used to consider a higher number of catchments to test the methodology, reducing the computational time.

The hyetographs scaled with the ARF for the entire river basin area must be attributed to each sub-basin. Even if a fully distributed model can better describe the hydrological processes involved in runoff generation in a storm, the goal of the ARF is to spatially scale an event on a given area. Moreover, without the use of the ARF, the use of a fully distributed model shows a drawback, consisting in the relative position between the rainfall raster and the river basin. When a real event is modeled in the same location where it occurred already in the past, the position of the rainfall raster is automatically obtained with an interpolation of the rain gauges in their position. Nevertheless, when a meteorological event is tested over a different location, the subjective choice of the distance between the center of the event and the river basin barycenter must be introduced. With a distributed model, there are more combinations for the same raster, with different cells that lie in or outside the river basin. Lastly, this procedure is designed to be applied easily by decision-makers that assess and manage flood risks. For all these reasons, the software used in this study to model both the design and the real events is HEC-HMS (USACE, 2013) because it is a well-known and widely

used semi-distributed hydrological model. Nonetheless, almost all semi-distributed hydrological model can be used to replicate this methodology.

2.5 | Comparison of the design and short-duration events

The comparison between design event and SDEs discharges is complete by looking at the peaks of the hydrographs. To summarize the results of this comparison, an index called delta flash flood design index, ΔFFD , is introduced as:

$$\Delta\text{FFD} = \frac{\sum_1^{ne} q_{\text{SDE}}/ne}{q_{200}} \quad (8)$$

The ΔFFD index represents the ratio between the mean of the peak discharges q_{SDE} , of the selected SDEs, and the peak of the design discharge, in this study the 200-year flood. If ΔFFD is greater than 1 in a river basin, the design discharge of that river basin underestimates the flash flood risk.

3 | APPLICATION OF THE SDE HYETOGRAPHS ON NORTHERN TUSCANY

3.1 | Dataset and short-duration events—SDEs Identification

The dataset of this work has been provided by the District River Basin Authority of Northern Apennine (“Autorità di Bacino Distrettuale dell’Appennino Settentrionale” in Italian) and it covers the period 2002–2017. In the study, there are 191 rain gauges of the Tuscany Region (central Italy) under the “Arno River Basin Authority” that covers an area of 16,000 km² (Figure 3). The time resolution of the rainfall data is 15 min. In Tuscany, extreme rainfall depths are greater along the coast. This is evident looking at the design rainfalls with a given return period and duration, as it is shown with the 200 years flood in the duration of 3 h (Figure 3). In the region, the 200-year flood event is commonly used in the hydrological design. The most intense SDEs recorded near the coast would produce floods greater than the design one if they are tested on river basins in the inner parts of Tuscany. Consequently, the analysis is divided into two different datasets, that is, STAs: the real events that occurred near the sea are tested on the coastal river basins where the design rainfall depths are comparable with the coastal

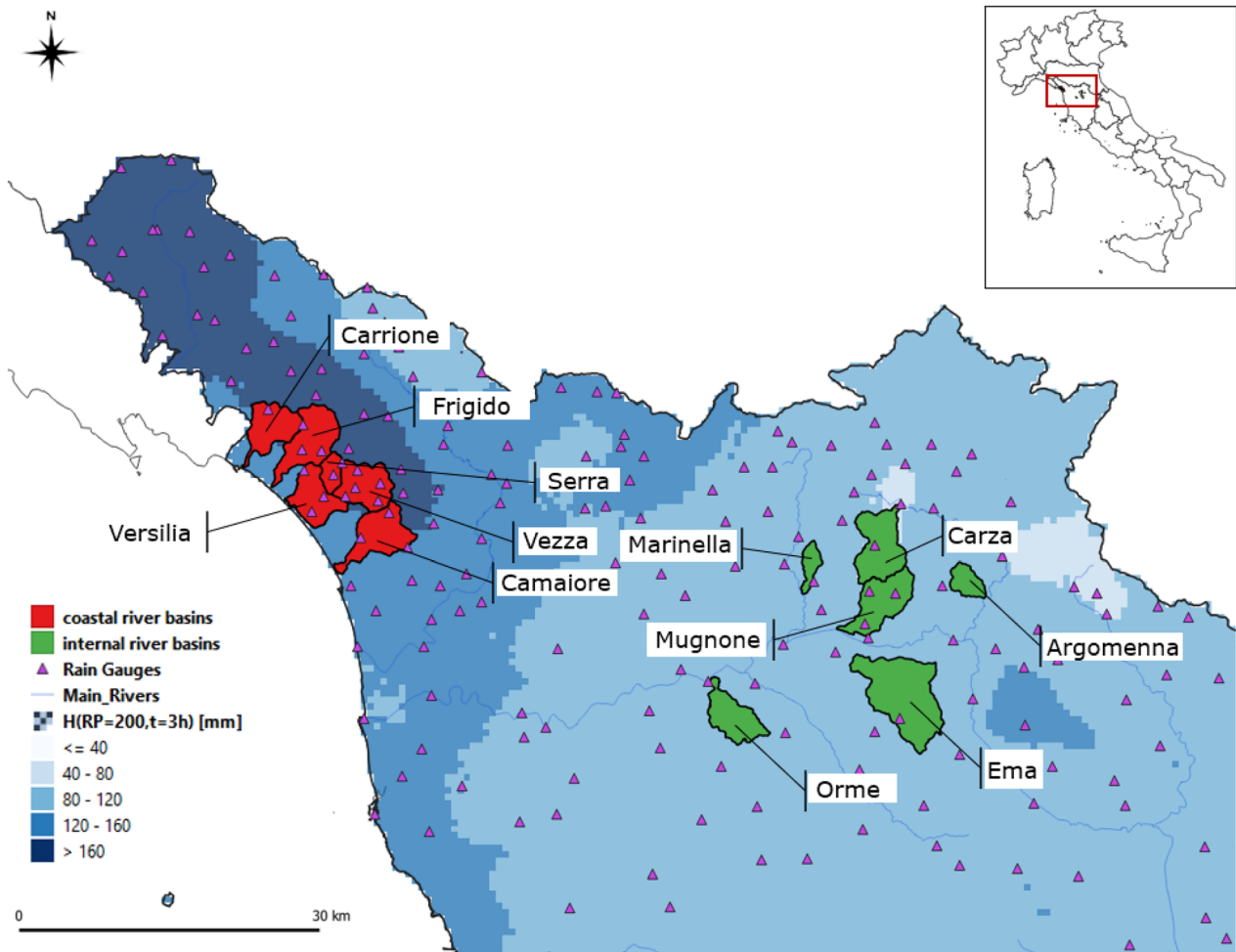


FIGURE 3 Rain gauge network and spatial distribution of the design rainfall depths H for a return period of 200 years and a duration of 3 h in the study area. Catchments located in the coastal area are in red. Catchments located in the inner area are in green

TABLE 1 Short-duration events, SDEs, for the inner part of the region

Name	Rain gauge	Date	h_{ev} (mm)	h_{200} (mm)	h_n
ISDE1	Cavallina	09/20/2014	112.6	83.4	1.35
ISDE2	Certaldo	09/18/2010	108.8	92.5	1.18
ISDE3	Poggibonsi	06/05/2011	96.2	96.8	0.99
ISDE4	Radda in Chianti	08/31/2012	100.2	104.4	0.96
ISDE5	Vinci	10/05/2010	90.8	98.2	0.92

SDEs. The real events in the inner part of the region have been tested on the internal river basins.

After rainfall data analysis, the most intense SDEs have been selected for the two groups with a Peak Over Threshold on the normalized rainfall depths (see Section 2.1). The internal SDEs are named ISDE and are presented in Table 1, the coastal short duration are named CSDE and are presented in Table 2. The tables report the name of the rain gauge that has the maximum within the event, the date of the day in which the event began, maxima rainfall for a duration of 3 h, h_{ev} , in

descending order of normalized depths, h_n . The normalization is done with the design rainfall with a return period (RP) of 200 years, h_{200} .

The average design rainfall with a RP of 200 years is 95 mm for the rain gauges in the inner part of the region (Table 1) and 135 mm for the coastal ones (Table 2). An event with 150 mm in 3 h represents almost a 200-year event in the coastal area and has RP that is greater than a 500 years event in the inner part of the region. The two river basin groups are summarized in Tables 3 and 4 and are shown in Figure 3.

Name	Rain gauge	Date	h_{ev} [mm]	h_{200} [mm]	h_n
CSDE1	Valle Benedetta	09/09/2017	235.0	137.7	1.71
CSDE2	Bocca d'Arno	10/26/2004	143.0	119.9	1.19
CSDE3	Pisa (Facoltà di Agraria)	08/24/2015	143.8	131.0	1.10
CSDE4	Gombitelli	07/21/2014	150.0	150.4	1.00

TABLE 2 Short-duration events, SDEs, for the coastal part of the region

TABLE 3 Set of the river basins in the inner parts of Tuscany

Name	A (km ²)	t_c (h)	Nearest rain gauge	h_{200}
Marinella	14.7	1.9	Calenzano	90.0
Argomenna	20.3	1.6	S. Brigida all'Opaco	97.1
Orme	47.5	3.1	Empoli	96.0
Mugnone	60.8	2.8	Caldine	94.2
Carza	66.7	2.9	Vaglia	78.4
Ema	112.3	4.0	Strada in Chianti	98.4

TABLE 4 Set of the river basins near the Tyrrhenian Sea

Name	A (km ²)	t_c (h)	Nearest rain gauge	h_{200}
Serra	16.0	1.5	Cerreto	162.6
Carrione	49.2	2.7	Torano	162.0
Veza	52.0	3.1	Terrinca	189.7
Camaioire	58.8	3.1	Camaioire	147.8
Frigido	62.7	3.5	Canevara	171.6
Versilia	115.1	4.8	Strettoia	159.4

Six river basins have been chosen with different catchment areas for each group to analyze the relationship between flash floods and design events for different small river basins areas and time of concentrations (t_c). The nearest rain gauge is included in the tables, showing the significant difference in the design rainfall depths between the two STAs (also in this case h_{200} refers to the duration of 3 h).

The average 200 year design rainfall in the duration of 3 h (h_{200}) is 92.4 mm for the internal river basin group and 165.5 mm for the coastal one.

Figure 4 shows as an example the spatial distribution and the rain gauges involved in the CSDE4, occurred on 21 July 2014 (Table 2). Eleven rain gauges recorded a total rainfall greater than 1 mm during the event. The rainfall spatial distribution was obtained with the IDW method. The maximum rainfall depth in 3 h recorded by the Gombitelli rain gauge was 150 mm. The Freddana river basin had a flash flood during this event.

3.2 | Hydrological models: Comparison between design and SDE hyetographs

A semi-distributed hydrological model is used (Section 2.4). The simulations are made at an event temporal scale, rather than the use of a continuous hydrological model, as it is meant to be applied during the design phase. Each SDE hyetograph has the shape of the hyetograph recorded at the rain gauge with the maximum rainfall depth in the storm and can be scaled with all the ARFs for the different river basin extensions. Figure 5 shows as an example the ISDE1 hyetograph (Table 1) recorded by the Cavallina rain gauge and the ARFs associated with the event.

The example also shows the same event modeled on the Carza river basin (internal river basin in Table 2). Since the entire river basin area is 67 km², the hyetograph recorded by the rain gauge with the maximum depth (Figure 5 left) is scaled with an ARF of 0.73 and then is applied to each subbasin. Therefore, rainfall depths recorded in the rain gauge are reduced by 27%, considering the spatial distribution of the event over the given area.

The design hydrographs have been modeled using the rainfall depths obtained with the intensity-duration-frequency curves developed by (Caporali et al., 2018) as input data, as they are used by professionals and decision-makers in the Tuscany Region. In this case, the rainfall depth has been obtained for each river basin by Equation (9).

$$h_{RP,t_c} = a_{RP} * t_c^{n_{RP}} \quad (9)$$

where t_c is the time of concentration of a generic river basin, h_{RP,t_c} is the design rainfall depth for the return period RP and the duration t_c , and a_{RP} and n_{RP} are the intercept and the slope of the intensity-duration-frequency linear curve in the Gumbel probability plot for a given return period, respectively. The temporal distribution of the design storm is assigned with a triangular shape because it is the peak hyetograph commonly used in the region: the peak timing corresponds to $0.4t_c$, the magnitude of the peak has an intensity equal to double the constant intensity hyetograph. The loss method used

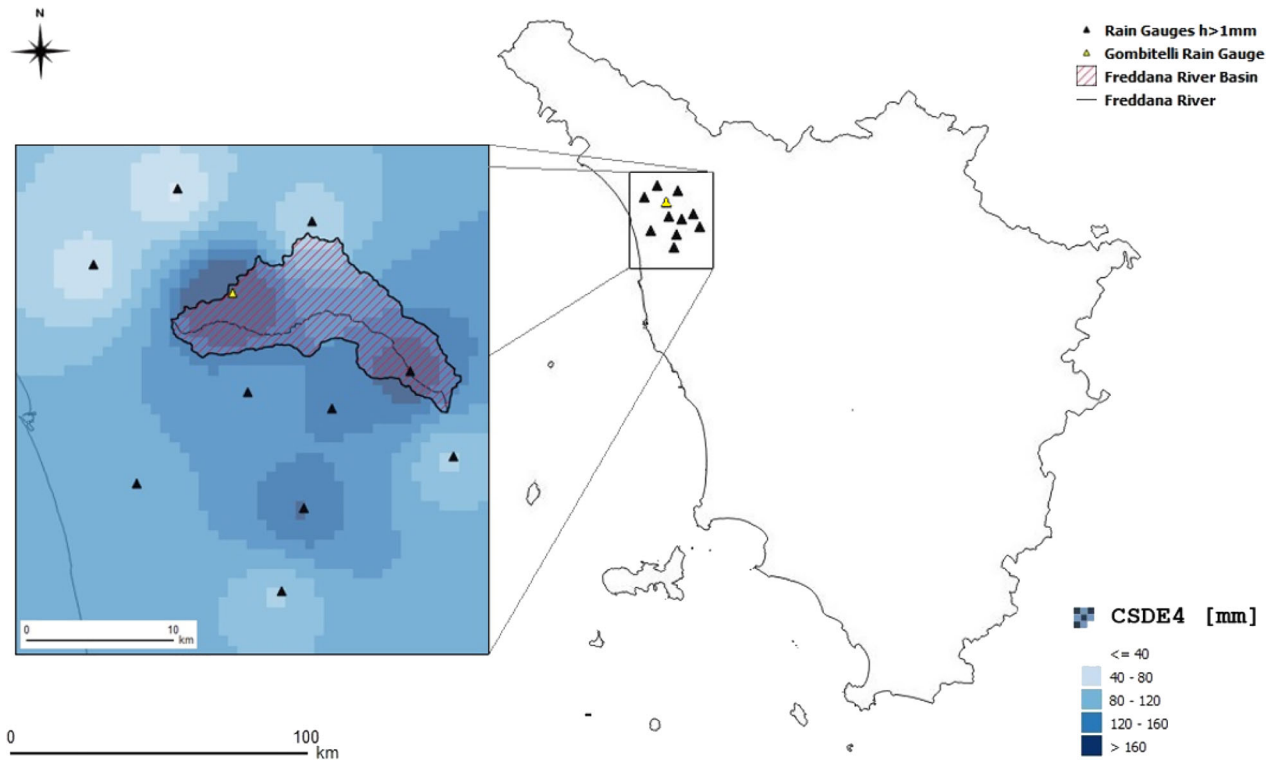
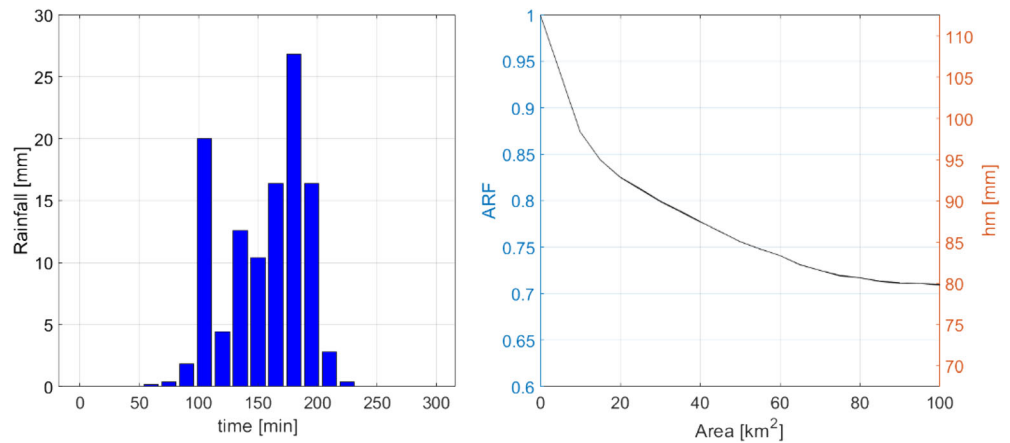


FIGURE 4 Rain gauges and rainfall raster of CSDE4 (coastal short duration event)

FIGURE 5 ISDE1 (internal short-duration event) hyetograph and areal reduction factors associated to the event



in the hydrological model for both the design storms and the SDEs event is SCS curve number (CN), since also in this case, it is commonly used in the study area by the professionals. Therefore, the runoff R is estimated as:

$$R = \frac{(P - 0.2S)^2}{(P + 0.8S)} \quad (10)$$

where P is the rainfall, and S is the potential maximum retention after runoff begins, which depends on the CN value as in the Equation (11).

$$S = 254 \left(\frac{100}{CN} - 1 \right) \quad (11)$$

The CN is obtained combining the information regarding the soil type with the land use obtained with the Corine Land Cover 2013. The antecedent soil moisture condition (AMC) is assumed to be the same in the comparison between the design events and the SDEs events. The AMC is assumed to be the mean condition, considered with the CNII. The transform method is the SCS Unit Hydrograph in which the lag time has been estimated as the 60% of each subbasin time of concentrations. The

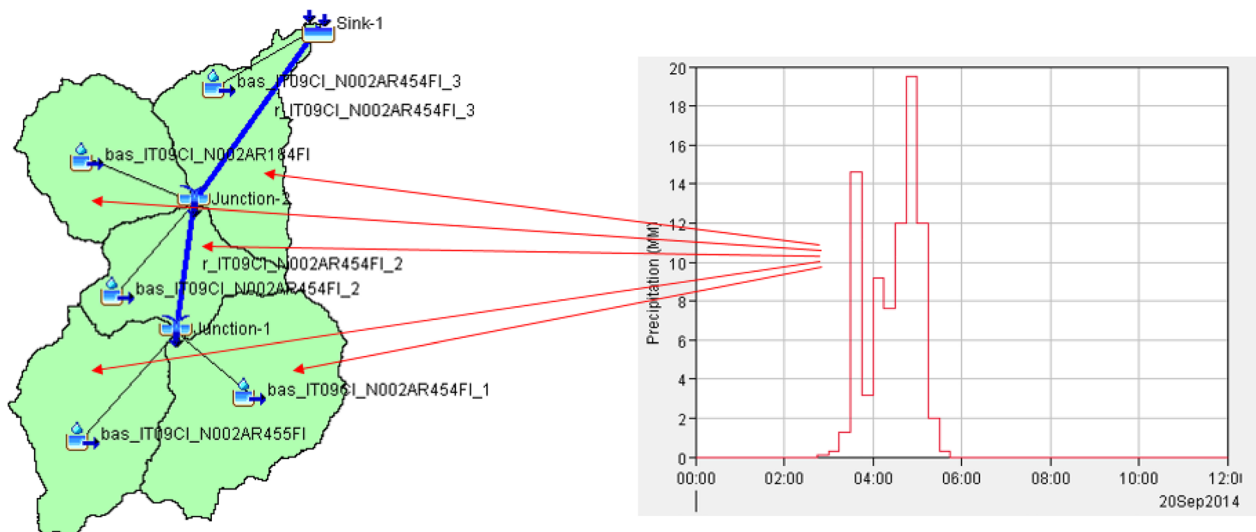


FIGURE 6 Carza river basin model: ISDE1 (internal short-duration event) hyetograph is scaled on the entire river basin area and it is the input of all the subbasins

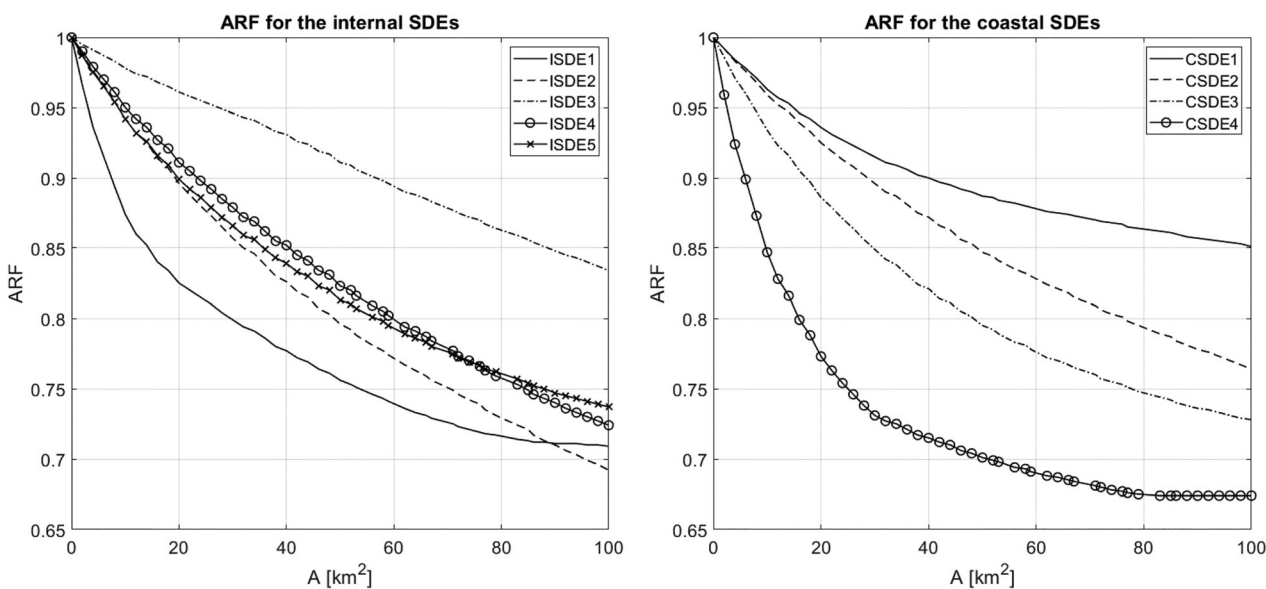


FIGURE 7 Areal reduction factors associated to the internal short-duration events (left) and to the coastal short-duration events (right)

model is used without a calibration for two reasons: almost all the examined river basins are ungauged and no streamflow data are available; the model estimate only the difference between the SDEs and the design event peaks with the same initial soil moisture conditions.

4 | RESULTS

The ARFs associated with all the 9 events considered in the study are shown in Figure 7 for the internal events on the left and for the coastal events on the right. The distribution of the ARFs with respect to the river basin

size A is shown just until a river basin extension of 100 km^2 since this study focuses on small river basins and concentrated storms in the spatial scale.

The results of the hydrological modeling are shown for the river basins in the internal STA (Figure 8) and coastal STA (Figure 9) of Northern Tuscany. The peak discharge of the 200-year design storm of each river basin (red line) is compared with the peaks of the hydrographs generated by the SDEs (blue points) and with the mean of all the peaks obtained with the SDEs (blue dotted line).

The ΔFFD index (Section 2.5) has been evaluated for each river basin, and it is shown respect to the river basin area for the two STAs in Figure 10: the green dots

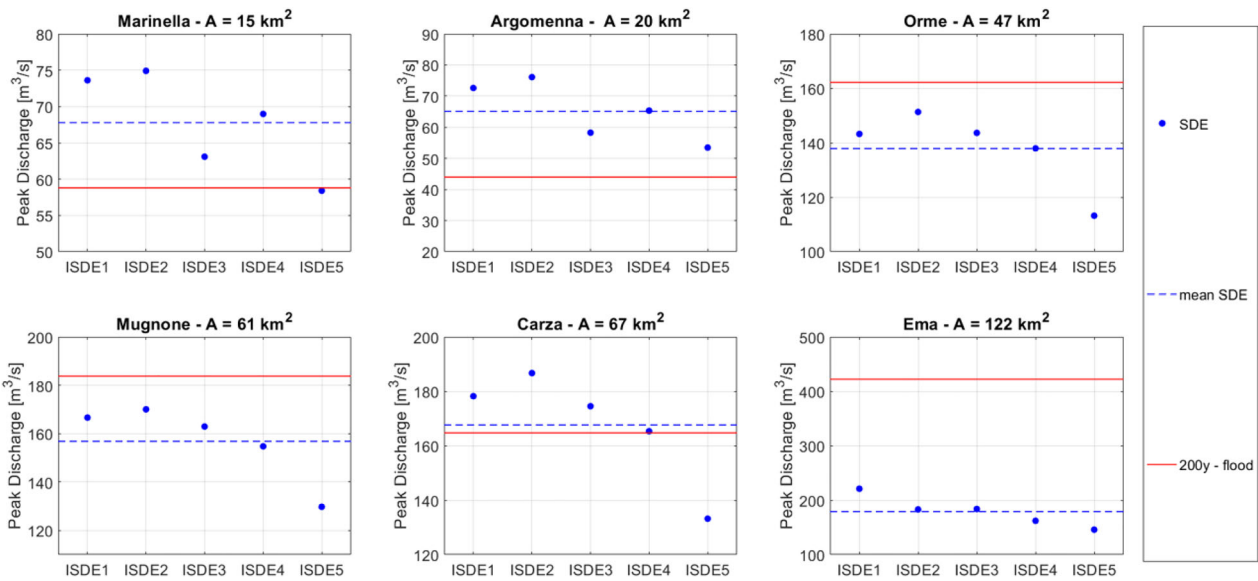


FIGURE 8 Results of all short-duration events occurred inland (Table 1) in the set of internal river basins. The red line shows the 200-year design storm flood peak, the blue points represent the peaks of the short-duration events (SDEs), and the dotted blue line the mean of the SDEs peaks

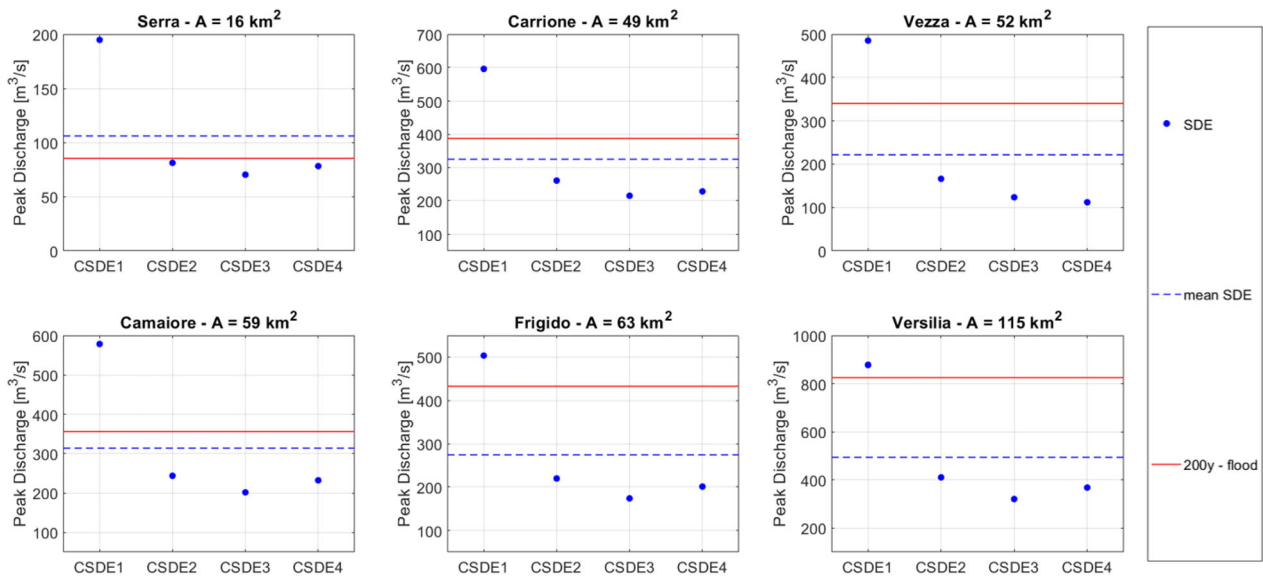


FIGURE 9 Results of all short-duration events occurred near the coast (Table 2) in the set of coastal river basins. The red line shows the 200-year design storm flood peak, the blue points represent the peaks of the short-duration events (SDEs), and the dotted blue line the mean of the SDEs peaks

represent the index for the internal river basins, the red dots for the coastal river basins.

5 | DISCUSSION

The use of past SDEs as synthetic hyetographs can be a strategy to better understand the flash flood hazard of small river basins. The use of ARFs guarantees that the

past events can be modeled also in other locations. The procedure proposed in this article ensures that each SDE is spatially analyzed, and a single ARF is obtained for each river basin size. Each SDE has its own spatial distribution and the ARF values associated with each event show a different behavior as the river basin area increases, as in Figure 7. Some ARFs scale almost linearly with the river basin area, and this could be due to the weighting parameter used in the IDW. Nevertheless,

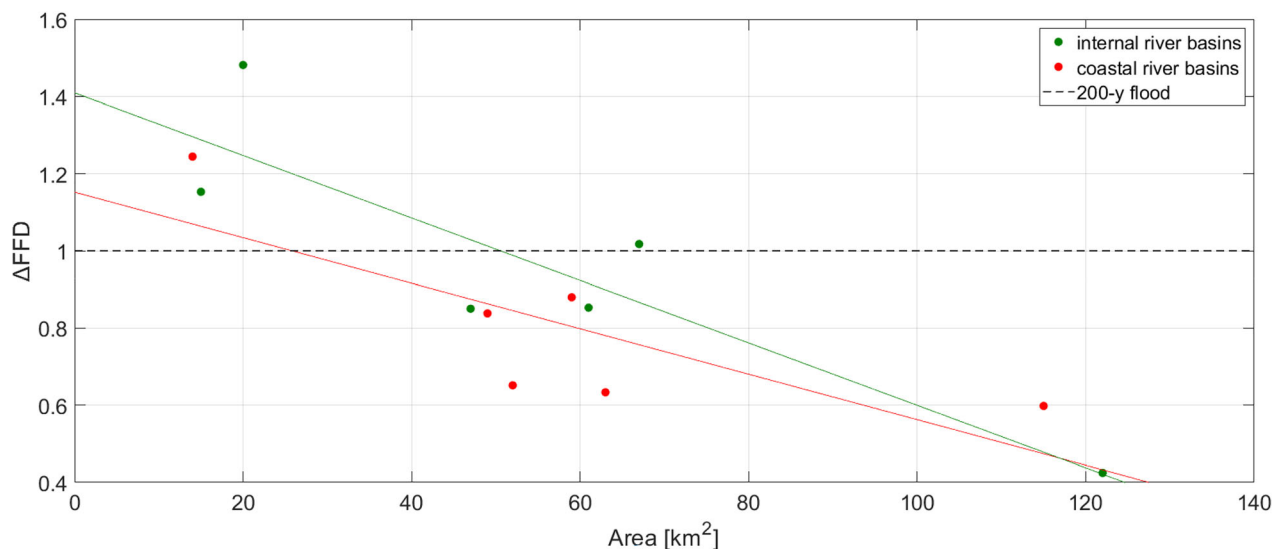


FIGURE 10 Delta flash flood design index with respect to the river basin area for the internal river basins and the coastal river basins

almost all the SDEs lose 30% of their intensity in just 100 km². This result agrees with some other studies that show how SDEs have more sharply decreasing ARFs with increasing areas than long-duration events, and this is probably due to the convective origin of these storms (NERC, 1975; Ramos et al., 2005).

In Northern Tuscany, design discharges relate with flash flood events with different patterns depending on the zone and on the river basin size. Considering the inner part of the region, the design discharges of the internal river basins are generally smaller than the magnitude of the hydrographs produced by the ISDEs for river basins smaller than 30 km² (upper part of Figure 8). The hydraulic risk assessment according to the 200 year design event is nonprecautionary against the flash flood hazards in such river basins. On the contrary, when greater river basins are considered, the design flood seems to be precautionary also against the SDEs, except for the Carza river basin, that show a ΔFFD slightly higher than one. Even when the coastal area is considered, design events underestimate the flash flood risk in the river basins with an area generally less than 30 km². Indeed, the Serra River basin shows a ΔFFD greater than one (Figure 9). Nevertheless, the design storms obtained according to the regional frequency analysis of the Tuscany Region (Caporali et al., 2018) seems to be more adequate also against the flash flood risks in the coastal area. Indeed, there are three river basins in the inner part of the region with a design discharge that underestimates the flash flood risk (Figure 10), while along the coast only the smallest river basin has a ΔFFD greater than one. There are several aspects that affect the relation between design and SDEs

peaks, such as the rain gauges time series length and the gauging site density near a given river basin. For these reasons the linear regression of ΔFFD with respect to the river basin area in Figure 10 has not been derived to obtain a factor also for other river basins. The red and the green line in Figure 10 emphasize how the coastal river basins generally appear to be safer against the flash flood risk than the internal river basins for all the river basin extensions. According to some findings in the literature, convective storms are more frequent near the coast and flash flood intensity decreases when moving inland (Gaume et al., 2009). Nevertheless, this study points out that a greater frequency and magnitude of extreme SDEs along the coast can partially explain why also the design rainfalls are greater and precautionary against flash flood risk in that region. Indeed, just a single coastal short-duration event (CSDE1) exceeds the design hydrograph of all the river basins along the coast. Nevertheless, this event corresponds to the flash flood occurred in Livorno during the night between the 9th and 10th September 2017, which has been proved to have an extremely rare intensity, if compared with design event, also in other studies (Arrighi & Castelli, 2020; Ricciardelli et al., 2018).

6 | CONCLUSIONS

Evaluating if the design discharge commonly used for the flood risk assessment can underestimate the flood peak discharges of extreme SDEs in small river basins is very important for decision-making. This study focused on determining a methodology to characterize hyetographs

of SDEs that can be applied for the flash flood assessment at the river basin scale, to identify those river basins in which the design discharges underestimate that risk. A simple methodology that considers the spatial distribution of past rainfall events has been proposed using the ARFs. The SDE hyetographs have been used as input data in a semi-distributed hydrological model for a set of small river basins in Northern Tuscany to analyze the impacts of the possible consequent flash floods. The results have underlined that the 200-year flood, commonly used in the flood risk assessment in the region, should be combined with the analysis of the response of a river basin to intense SDEs, to be more precautionary against the flash flood risk. This is important for small river basins with an area generally less than 30 km².

The results cannot be extended to other regions, but the simplicity of the proposed method could bring some decision-makers to replicate the methodology in other case studies for a better evaluation of flash flood hazards at the river basin scale. The procedure is not meant to replace the classical modeling with design events, though it seeks to be a methodology that could be used alongside the classic hydraulic risk evaluation to improve the flash flood risk assessment. If the design flood is over the mean of the SDEs peaks, the flash flood hazard is considered just using the classical approach with the design flood for that river basin. On the contrary, the decision-makers could consider the additional risk due to flash flood events by using the ΔFFD index.

DATA AVAILABILITY STATEMENT

Data sharing is not applicable to this article as no new data were created or analyzed in this study.

ORCID

Marco Lompi  <https://orcid.org/0000-0003-2970-168X>

Enrica Caporali  <https://orcid.org/0000-0001-6389-3801>

Luis Mediero  <https://orcid.org/0000-0002-9346-6592>

REFERENCES

- Ali, K., Bajracharyar, R. M., & Raut, N. (2017). Advances and challenges in flash flood risk assessment: A review. *Journal of Geography & Natural Disasters*, 7(2), 1–6. <https://doi.org/10.4172/2167-0587.1000195>
- Arrighi, C., & Castelli, F. (2020). The 2017 flash flood of Livorno (Italy): Lessons learnt from an exceptional hydrologic event. In F. Fernandes, A. Malheiro, & H. Chaminé (Eds.), *Advances in natural hazards and hydrological risks: Meeting the challenge. Advances in science, technology & innovation (IEREK interdisciplinary series for sustainable development)*. Springer. https://doi.org/10.1007/978-3-030-34397-2_23
- Bacchi, B., & Ranzi, R. (1996). On the derivation of the areal reduction factor of storms. *Atmospheric Research*, 42(1–4), 123–135. [https://doi.org/10.1016/0169-8095\(95\)00058-5](https://doi.org/10.1016/0169-8095(95)00058-5)
- Barbero, G., Moisélo, U., & Todeschini, S. (2014). Evaluation of the areal reduction factor in an urban area through rainfall records of limited length: A case study. *Journal of Hydrologic Engineering*, 19(11), 1–10. [https://doi.org/10.1061/\(ASCE\)HE.1943-5584.0001022](https://doi.org/10.1061/(ASCE)HE.1943-5584.0001022)
- Berg, P., Moseley, C., & Haerter, J. O. (2013). Strong increase in convective precipitation in response to higher temperatures. *Nature Geoscience*, 6(3), 181–185. <https://doi.org/10.1038/ngeo1731>
- Blöschl, G., Hall, J., Viglione, A., Perdigão, R. A. P., Parajka, J., Merz, B., Lun, D., Arheimer, B., Aronica, G. T., Bilbashi, A., Boháč, M., Bonacci, O., Borga, M., Čanjevac, I., Castellarin, A., Chirico, G. B., Claps, P., Frolova, N., Ganora, D., ... Živković, N. (2019). Changing climate both increases and decreases European river floods. *Nature*, 573(7772), 108–111. <https://doi.org/10.1038/s41586-019-1495-6>
- Cao, C., Xu, P., Wang, Y., Chen, J., Zheng, L., & Niu, C. (2016). Flash flood hazard susceptibility mapping using frequency ratio and statistical index methods in coalmine subsidence areas. *Sustainability (Switzerland)*, 8(9), 948. <https://doi.org/10.3390/su8090948>
- Caporali, E., Chiarello, V., & Petrucci, A. (2018). Regional frequency analysis and geospatial modeling for design storm estimates in the Arno river basin (Italy). *Environmental and Ecological Statistics*, 25(1), 31–52. <https://doi.org/10.1007/s10651-018-0399-1>
- Caporali, E., Lompi, M., Pacetti, T., Chiarello, V., & Fatichi, S. (2021). A review of studies on observed precipitation trends in Italy. *International Journal of Climatology*, 41(S1), E1–E25. <https://doi.org/10.1002/joc.6741>
- Dawod, G. M., Mirza, M. N., & Al-Ghamdi, K. A. (2011). GIS-based spatial mapping of flash flood Hazard in Makkah City, Saudi Arabia. *Journal of Geographic Information System*, 3(3), 225–231. <https://doi.org/10.4236/jgis.2011.33019>
- De Michele, C., Kottegoda, N. T., & Rosso, R. (2001). The derivation of areal reduction factor of storm rainfall from its scaling properties. *Water Resources*, 37(12), 3247–3252.
- Dougherty, E., & Rasmussen, K. L. (2021). Variations in flash flood-producing storm characteristics associated with changes in vertical velocity in a future climate in the Mississippi River basin. *Journal of Hydrometeorology*, 22(3), 671–687. <https://doi.org/10.1175/JHM-D-20-0254.1>
- Esposito, G., Matano, F., & Scepi, G. (2018). Analysis of increasing flash flood frequency in the densely urbanized coastline of the campi flegrei volcanic area. *Italy. Frontiers in Earth Science*, 6-(June), 1–17. <https://doi.org/10.3389/feart.2018.00063>
- Faccini, F., Luino, F., Paliaga, G., Sacchini, A., Turconi, L., & de Jong, C. (2018). Role of rainfall intensity and urban sprawl in the 2014 flash flood in Genoa City, Bisagno catchment (Liguria, Italy). *Applied Geography*, 98, 224–241. doi:10.1016/j.apgeog.2018.07.022
- Faccini, F., Luino, F., Sacchini, A., & Turconi, L. (2015). The 4th October 2010 flash flood event in Genoa Sestri Ponente (Liguria, Italy). *Disaster Advances*, 8, 1–14.
- Foufoula-Georgiou, E. (1989). A probabilistic storm transposition approach for estimating exceedance probabilities of extreme precipitation depths. *Water Resources Research*, 25, 799–815.
- Franchini, M., Helmlinger, K. R., Foufoula-Georgiou, E., & Todini, E. (1996). Stochastic storm transposition coupled with rainfall runoff modeling for estimation of exceedance probabilities of design floods. *Journal of Hydrology*, 175(1–4), 511–532.

- Gaume, E., Bain, V., Bernardara, P., Newinger, O., Barbuc, M., Bateman, A., Blaškovičová, L., Blöschl, G., Borga, M., Dumitrescu, A., Daliakopoulos, I., Garcia, J., Irimescu, A., Kohnova, S., Koutroulis, A., Marchi, L., Matreata, S., Medina, V., Preciso, E., ... Viglione, A. (2009). A compilation of data on European flash floods. *Journal of Hydrology*, *367*(1–2), 70–78. <https://doi.org/10.1016/j.jhydrol.2008.12.028>
- Kim, J., Lee, J., Kim, D., & Kang, B. (2019). The role of rainfall spatial variability in estimating areal reduction factors. *Journal of Hydrology*, *568*(October 2018), 416–426. <https://doi.org/10.1016/j.jhydrol.2018.11.014>
- Kourgialas, N. N., & Karatzas, G. P. (2011). Gestion des inondations et méthode de modélisation sous SIG pour évaluer les zones d'aléa inondation-une étude de cas. *Hydrological Sciences Journal*, *56*(2), 212–225. <https://doi.org/10.1080/02626667.2011.555836>
- Koutsoyiannis, D., & Foufoula-Georgiou, E. (1993). A scaling model of a storm hyetograph. *Water Resources Research*, *29*(7), 2345–2361. <https://doi.org/10.1029/93WR00395>
- Lenderink, G., & Van Meijgaard, E. (2008). Increase in hourly precipitation extremes beyond expectations from temperature changes. *Nature Geoscience*, *1*(8), 511–514. <https://doi.org/10.1038/ngeo262>
- Llasat, M. C., Marcos, R., Turco, M., Gilabert, J., & Llasat-Botija, M. (2016). Trends in flash flood events versus convective precipitation in the Mediterranean region: The case of Catalonia. *Journal of Hydrology*, *541*(October), 24–37. <https://doi.org/10.1016/j.jhydrol.2016.05.040>
- Marchi, L., Borga, M., Preciso, E., & Gaume, E. (2010). Characterisation of selected extreme flash floods in Europe and implications for flood risk management. *Journal of Hydrology*, *394*(1–2), 118–133. <https://doi.org/10.1016/j.jhydrol.2010.07.017>
- Mogil, H. M., Monro, J. C., & Groper, H. S. (1978). NWS's flash flood warning and disaster preparedness programs. *Bulletin of the American Meteorological Society*, *59*(6), 690–699. [https://doi.org/10.1175/1520-0477\(1978\)059<0690:nffwad>2.0.co;2](https://doi.org/10.1175/1520-0477(1978)059<0690:nffwad>2.0.co;2)
- Natural Environment Research Council (NERC) (1975). Flood Studies Report. Vol. 1, London.
- Nnadi, F. N., Kline, F. X., Wray, H. L., & Wanielista, M. P. (1999). Comparison of design storm concepts using continuous simulation with short duration storms. *Journal of the American Water Resources Association*, *35*(1), 61–72. <https://doi.org/10.1111/j.1752-1688.1999.tb05452.x>
- Pavlovic, S., Perica, S., St Laurent, M., & Mejia, A. (2016). Intercomparison of selected fixed-area areal reduction factor methods. *Journal of Hydrology*, *537*, 419–430. <https://doi.org/10.1016/j.jhydrol.2016.03.027>
- Ramos, M. H., Creutin, J.-D., & Leblois, E. (2005). Visualization of storm severity. *Journal of Hydrology*, *315*(1–4), 295–307.
- Ricciardelli, E., Di Paola, F., Gentile, S., Cersosimo, A., Cimini, D., Gallucci, D., Gherardi, E., Larosa, S., Nilo, S. T., Ripepi, E., Romano, F., & Viggiano, M. (2018). Analysis of Livorno heavy rainfall event: Examples of satellite-based observation techniques in support of numerical weather prediction. *Remote Sensing*, *10*(10), 408–430. <https://doi.org/10.3390/rs10101549>
- Saharia, M., Kirstetter, P.-E., Vergara, H., Gourley, J. J., Hong, Y., & Giroud, M. (2017). Mapping flash flood severity in the United States. *Journal of Hydrometeorology*, *18*(2), 397–411. <https://doi.org/10.1175/jhm-d-16-0082.1>
- Sivapalan, M., & Blöschl, G. (1998). Transformation of point rainfall to areal rainfall: Intensity–duration–frequency curves. *Journal of Hydrology*, *204*(1–4), 150–167.
- Svensson, C., & Jones, D. A. (2010). Review of methods for deriving areal reduction factors. *Journal of Flood Risk Management*, *3*(3), 232–245. <https://doi.org/10.1111/j.1753-318X.2010.01075.x>
- USACE USACoE. (2013) Hydrologic modeling system HEC-HMS, user's manual, version 4.0.
- Venugopal, V., Foufoula-Georgiou, E., & Sapozhnikov, V. (1999). Evidence of dynamic scaling in space-time rainfall. *Journal of Geophysical Research Atmospheres*, *104*(D24), 31599–31610. <https://doi.org/10.1029/1999JD900437>
- Wright, D. B., Yu, G., & England, J. F. (2020). Six decades of rainfall and flood frequency analysis using stochastic storm transposition: Review, progress, and prospects. *Journal of Hydrology*, *585*, 124816. <https://doi.org/10.1016/j.jhydrol.2020.124816>
- Zhang, Y., Wang, Y., Chen, Y., Liang, F., & Liu, H. (2019). Assessment of future flash flood inundations in coastal regions under climate change scenarios—A case study of Hadahe River basin in northeastern China. *Science of the Total Environment*, *693*, 133550. <https://doi.org/10.1016/j.scitotenv.2019.07.356>

How to cite this article: Lompi, M., Caporali, E., Mediero, L., & Mazzanti, B. (2022). Improving flash flood risk assessment using a simple approach for extreme rainfall scaling and storms transposition. *Journal of Flood Risk Management*, e12796. <https://doi.org/10.1111/jfr3.12796>